# Comparison of the Thermodynamic Landscapes of Unfolding and Formation of the Energy Dissipative State in the Isolated Light Harvesting Complex II

Stefano Santabarbara,[†] Peter Horton,[‡] and Alexander V. Ruban[§*]

[†]Department of Physics, University of Strathclyde, Glasgow, Scotland, United Kingdom; [‡]University of Sheffield, Sheffield, United Kingdom; and [§]School of Biological and Chemical Sciences, Queen Mary University of London, London, United Kingdom

ABSTRACT In biochemistry and cell biology, understanding the molecular mechanisms by which physiological processes are regulated is regarded as an ultimate goal. In higher plants, one of the most widely investigated regulatory processes occurs in the light harvesting complexes (LHCII) of the chloroplast thylakoid membranes. Under limiting photon flux densities, LHCII harvests sunlight with high efficiency. When the intensity of incident radiation reaches levels close to the saturation of the photosynthesis, the efficiency of light harvesting is decreased by a process referred to as nonphotochemical quenching (NPQ), which enhances the singlet-excited state deactivation via nonradiative dissipative processes. Conformational rearrangements in LHCII are known to be crucial in promoting and controlling NPQ in vitro and in vivo. In this article, we address the thermodynamic nature of the conformational rearrangements promoting and controlling NPQ in isolated LHCII. A combined, linear reaction scheme in which the folded, quenched state represents a stable intermediate on the unfolding pathway was employed to describe the temperature dependence of the spectroscopic signatures associated with the chlorophyll fluorescence quenching and the loss of secondary structure motifs in LHCII. The thermodynamic model requires considering the temperature dependence of Gibbs free energy difference between the quenched and the unquenched states, as well as the unfolded and quenched states, of LHCII. Even though the same reaction scheme is adequate to describe the quenching and the unfolding processes in LHCII monomers and trimers, their thermodynamic characteristics were found to be markedly different. The results of the thermodynamic analysis shed light on the physiological importance of the trimeric state of LHCII in stabilizing the efficient light harvesting mode as well as preventing the quenched conformation of the protein from unfolding. Moreover, the transition to the quenched conformation in trimers reveals a larger degree of cooperativity than in monomers, explained by a small characteristic entropy ($\Delta H_q = 85 \pm 3$ kJ mol$^{-1}$ compared to $125 \pm 5$ kJ mol$^{-1}$ in monomers), which enables the fine-tuning of nonphotochemical quenching in vivo.

## INTRODUCTION

Nonphotochemical quenching (NPQ) of chlorophyll *a* (Chl *a*) fluorescence is a key regulatory process of the photosynthetic apparatus. By increasing the thermal dissipation of excited chlorophyll in photosystem II (PSII) antenna, NPQ downregulates its maximal photochemical efficiency in a manner similar to the classical feedback regulation of enzyme-catalyzed reactions. In vivo NPQ is controlled by several effectors, which lead to complex kinetics of quenching formation and relaxation (reviewed in (1–3)). The most rapidly formed and major component of NPQ is the so-called high-energy quenching. It is dependent upon the acidification of thylakoid lumen (1–3) and the function of PsbS subunit of PSII (e.g., (3)). Moreover, the extent of high-energy quenching and its relaxation kinetics are controlled by the stoichiometry of the xanthophyll cycle carotenoids, zeaxanthin and violaxanthin (reviewed in 1–4), which are bound exclusively to the major light-harvesting complex (LHCII) antenna (5–8). Violaxanthin is the most abundant xanthophyll cycle carotenoid in dark-adapted leaves (5–8). It can be replaced by zeaxanthin, which is produced by the enzymatic de-epoxidation of violaxanthin, when leaves are exposed to light (5–8).

The fluorescence yield of the main antenna complex of PSII, LHCII, can be modulated in vitro (e.g., (9–13)). When in the quenched state, LHCII shows spectroscopic signatures that are also found in thylakoid membranes (e.g., (14–16)). Moreover, fluorescence of LHCII in icosahedral crystals (12) is quenched and shows the same spectroscopic features as the aggregated complex (13). After investigation using time-resolved absorption spectroscopy, it was proposed that the quenching occurs through the transfer of the Chl *a* excited-singlet state to the forbidden S1 state of Lutein 1, which is bound at the interface of $\alpha$-helix A of LHCII (15). An alternative molecular mechanism for the quencher active in NPQ involves the formation of a charge-transfer complex between Chl *a* and one of the xanthophyll cycle carotenoids, zeaxanthin being the most likely candidate (17). Recent reports suggest that this type of quenching mechanism takes place preferentially in the so-called minor antenna complexes, chlorophyll protein complex (CP), namely, CP29, CP26, and CP24 (18,19).

Irrespective of the specific mechanism, the additional deactivation pathway for Chl *a* singlet-excited states requires modification of xanthophyll/chlorophyll coupling in the complex. For instance, the S1 state of lutein (and carotenoids in general) is geometrically forbidden, consequently having a very weak transition probability. Therefore, energy transfer

*Submitted March 28, 2009, and accepted for publication June 2, 2009.*

*Correspondence: a.ruban@qmul.ac.uk

Editor: Marilyn Gunner.



0006-3495/09/08/1188/10 $2.00

doi: 10.1016/j.bpj.2009.06.005

has to occur through relatively strong interactions between the electronic densities of the donor and the acceptor molecule (20,21). This kind of excited state transfer is extremely sensitive to even subtle rearrangements of the chromophores bound to LHCII. Similar considerations also apply to the proposed formation of a charge-transfer state (17–19,22). In the model proposed by Ruban et al. (15), the interaction between the S1 state of lutein and the excited state of Chl *a* is made possible because of conformational rearrangements in LHCII, which are likely to alter the distance and the mutual orientation between chromophores. Such pigment reconfigurations were demonstrated by monitoring the vibrational spectra of bound cofactors, which are very sensitive to even subtle modifications of pigment conformation (reviewed in (16)). The enhancement of some vibrational modes of neoxanthin is interpreted in terms of a twisted conformation of this carotene occurring during quenching (13–16). This shift of the resonance Raman frequencies of neoxanthin in isolated LHCII is almost identical to that observed as a result of NPQ in vivo (15). Although these studies address the conformational reorganization of bound cofactors in detail, very limited information is available on the conformational reorganization of the protein scaffold associated with the quenching. It has been suggested that such change in LHCII is promoted by thermo-optic effect associated with the heat release during the excited state relaxation of pigments, affecting their binding sites and the local surrounding (23,24). The transition between quenched and unquenched states of the complex has also been linked to a change in the oligomerization state of LHCII (reviewed in (1,2,16)). However, there is evidence that such quenching can be induced in monomeric and trimeric forms of the complex in the absence of protein aggregation (25,26).

The temperature dependence of the quenching formation kinetics in isolated LHCII complexes displays marked non-Arrhenius behavior (10,27,28). Deviations from the simple Arrhenius relationship are commonly observed for conformational reorganization of proteins taking place during folding in vitro (reviewed, e.g., (29–34)). Although it is expected that the conformational changes that occur during quenching in LHCII complexes are not as pronounced as those occurring in the folding process, these observations have led us to reinvestigate, in depth, the thermodynamics of the fluorescence quenching process in isolated LHCII complexes. The analysis reveal some key thermodynamic parameters of the transition from the unquenched to the quenched state of LHCII that uncover the role of the trimeric LHCII structure in the efficient control of light harvesting.

## MATERIALS AND METHODS

### Purification of LHCII

LHCII trimers were purified from spinach by separation on sucrose density gradient followed by iso-electrofocusing, as previously described (35). Monomers were obtained by the treatment of trimers with phospholipase, as described in Nussberger et al. (36).

### Spectroscopic analysis

Quenching of fluorescence in LHCII was obtained by dissolving either monomers or trimers in buffer containing $\beta$-*n*-dodecyl maltoside at a concentration lower than the critical micellar concentration (for details, see (27)). The kinetics of quenching was measured using a pulse-amplitude-modulated fluorimeter (model No. PAM100, Walz, Effeltrich, Germany); chromophores were excited at 650 nm and the emission collects at wavelengths longer than 690 nm. The kinetics of quenching was fitted as previously described (27). Circular dichroism (CD) measurements were performed before dissolving the sample in the low concentration buffer medium and after it has reached a steady-state level of quenching (as monitored by the fluorescence kinetics), using a model No. J810 spectropolarimeter (JASCO, Oklahoma City, OK). The temperature of the sample was controlled by either a circulating water bath (fluorescence emission) or a Peltier element. The change in CD intensity because of quenching was calculated by subtracting the spectrum of the quenched sample from that of the corresponding control. The $\Delta CD$ was also calculated at 211 nm to monitor the changes in the apo-protein secondary structure.

### Data analysis

#### *The model*

The detailed description of the choice of thermodynamic model employed to analyze the experimental data is given in Appendix S1 in the Supporting Material. In brief, two conformational transitions of LHCII need to be considered, that from the unquenched (folded) to the quenched (folded) state and that from the folded state(s) of the complex to the unfolded one. At least in the trimeric form of LHCII, the transitions to the quenched and to the unfolded forms of the complex are substantially sequential (27,28), so that they can be described by the following linear kinetic scheme:

$$LHC_{\mathrm{u}} \underset{K_{\mathrm{eq}}^{\mathrm{q}}}{\longleftrightarrow} LHC_{\mathrm{q}} \underset{K_{\mathrm{eq}}^{\mathrm{m}}}{\longleftrightarrow} LHC_{\mathrm{m}}. \qquad (1)$$

At steady state, the concentration of each form of the complex is proportional to their corresponding molar fraction being in unquenched ($\gamma_{\mathrm{u}}$), quenched ($\gamma_{\mathrm{q}}$), or denatured ($\gamma_{\mathrm{m}}$) state. The molar fractions can be expressed as a function of the quenching ($K_{\mathrm{eq}}^{\mathrm{q}}$) and melting ($K_{\mathrm{eq}}^{\mathrm{m}}$) equilibrium constants which are defined by the mass action law, and hence respective standard Gibbs free energy differences $\Delta G_{\mathrm{q}}^{\varnothing}(T)$ and $\Delta G_{\mathrm{m}}^{\varnothing}(T)$. The temperature dependence of $\Delta G_{\mathrm{q}}^{\varnothing}(T)$ (and $\Delta G_{\mathrm{m}}^{\varnothing}(T)$) with respect to a reference temperature $T_{\mathrm{q}}$ is described by the Gibbs-Helmholtz equation (e.g., (29–34)),

$$\Delta G_{\mathrm{q}}^{\varnothing}(T) = \Delta H_{\mathrm{q}}^{\varnothing}\left(1 - \frac{T}{T_{\mathrm{q}}}\right) + \Delta C_{\mathrm{p,q}}\left(T - T_{\mathrm{q}}\right) - \Delta C_{\mathrm{p,q}}\left(T \ln \frac{T}{T_{\mathrm{q}}}\right), \qquad (2)$$

where $\Delta H_{\mathrm{q}}^{\varnothing}$ and $\Delta S_{\mathrm{q}}^{\varnothing}$ are the standard quenching enthalpy and entropy difference at the reference temperature. $\Delta C_{\mathrm{p,q}}$ is the difference in specific heat capacity between the unquenched (relaxed) and the quenched form of the LHCII complex, which is considered as temperature-independent. An identical expression is used to describe the melting transition by substitution of the $q$ subscript with $m$.

### Analysis of the activation barrier

The temperature dependencies of the quenching kinetics are given by the Eyring-Evans equation,

$$k(T) = \kappa\frac{k_b T}{h} \times e^{-\frac{\Delta G^*(T)}{RT}}, \quad (3)$$

where $\kappa$ is the transmission coefficient (i.e., the probability that the reaction takes place from the transition state), $h$ is the Plank constant, $k_b$ is the Boltzmann constant, and $\Delta G_q^*(T)$, is the activation free energy difference. $\Delta G_q^*(T)$ for an endergonic reaction can be expressed as a linear combination of the free energies of activation of the reverse, exergonic reaction, $\Delta G_q^{\dagger}(T)$, and $\Delta G_q(T)$. $\Delta G_q^{\dagger}(T)$ is also described by the Gibbs-Helmholtz equation. Expressed in function of the temperature $T_q$ used to define$\Delta G_q(T)$ gives

$$\Delta G_q^{\dagger}(T) = \Delta H_q^{\dagger} - T\Delta S_q^{\dagger} + \Delta C_{p,q}^{\dagger}(T - T_q) - \Delta C_{p,q}^{\dagger}\left(T\ln\frac{T}{T_q}\right), \quad (4)$$

where $\Delta H_q{}^{\dagger}$ is the activation enthalpy difference, $\Delta C^{\dagger}{}_{p,q}$ is the differential heat capacity between the quenched form of the complex and the transition state, and $\Delta S_q{}^{\dagger}$ is the activation entropy difference. Similar treatments for the activation energy barrier have been discussed in protein folding and unfolding studies (e.g., (37–39)).

## Fitting procedure

The experimental results were fitted to the thermodynamic model by using a nonlinear least-square routine, minimizing $\chi^2$. To reduce the number of possible solutions and to increase the accuracy in estimation of the model parameters, the data were fitted globally. The stability of the fit solutions was tested as described by Beechem (40). To show the range of possible acceptable solutions, the levels of confidence associated with the fits are presented. Further details on the fit and error estimation procedure are given in Appendix S2 in the Supporting Material.

# RESULTS AND DISCUSSION

## Fitting the experimental data

The ability to induce fluorescence quenching in vitro provides a simple and reliable manner to study the NPQ process in a model system for which the experimental conditions can be carefully controlled. In an attempt to obtain a more complete picture of the thermodynamics underlying singlet-excited state quenching in LHCII, we have reinvestigated the temperature dependence of fluorescence quenching in the isolated complex. The temperature dependence of fluorescence quenching in LHCII was monitored either following the time-dependent decrease of fluorescence emission, which provides information relating to the kinetics and the activation barrier of the quenching process, or by recording the CD spectrum before and after the induction of quenching. The extent of fluorescence quenching and the quenched-minus-unquenched $\Delta CD$ signal are linearly correlated (e.g., (27)). The latter experiments provide information related to the steady-state populations of the quenched and unquenched (relaxed) state of the complex. The temperature-induced unfolding of the LHCII was shown to display similar behavior to the induction of quenching, albeit occurring at higher temperatures (27,28).

Fig. 1 shows the comparison of the temperature dependence of the CD signal associated with protein secondary structure (211 nm) and chromophore excitonic coupling (680 nm), recorded in monomers and trimers of LHCII. Fig. 2 shows

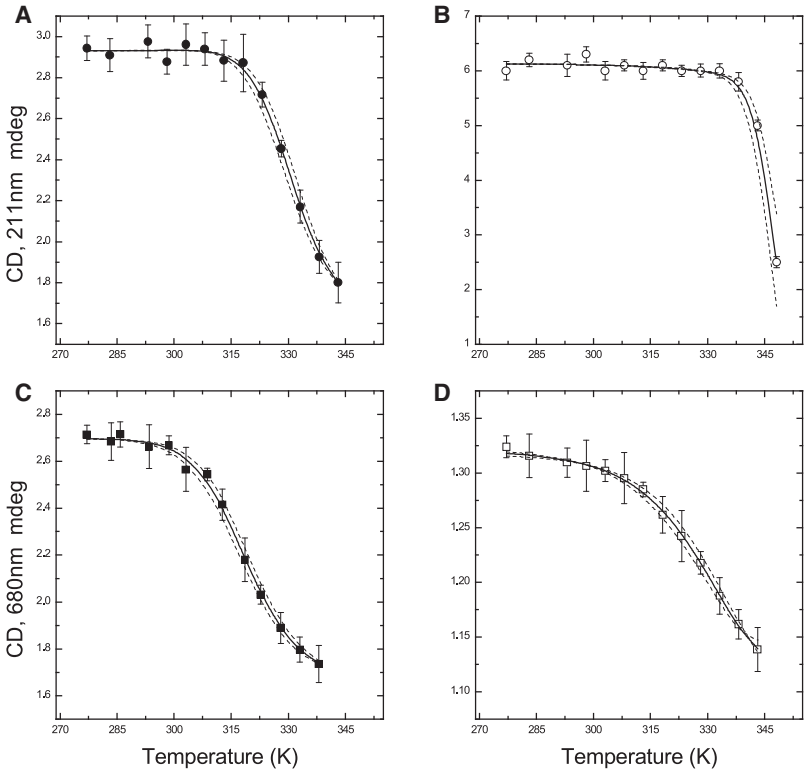


FIGURE 1 (*A* and *B*) Temperature dependence of steady-state unfolding of LHCII monomers (*A*) and trimers (*B*), measured as decrease in CD signal at 211 nm. (*C* and *D*) Temperature dependences of steady-state fluorescence quenching in LHCII monomers (*C*) and trimers (*D*), measured as decrease in CD signal at 680 nm. The error bars represent the standard deviation, over five independent replicates. (*Solid lines*) Fits obtained for the reaction scheme model described in the text. (*Dashed lines*) Confidence interval (within $2\sigma$). Reduced $\chi^2$ varied from 0.98 to 1.05.

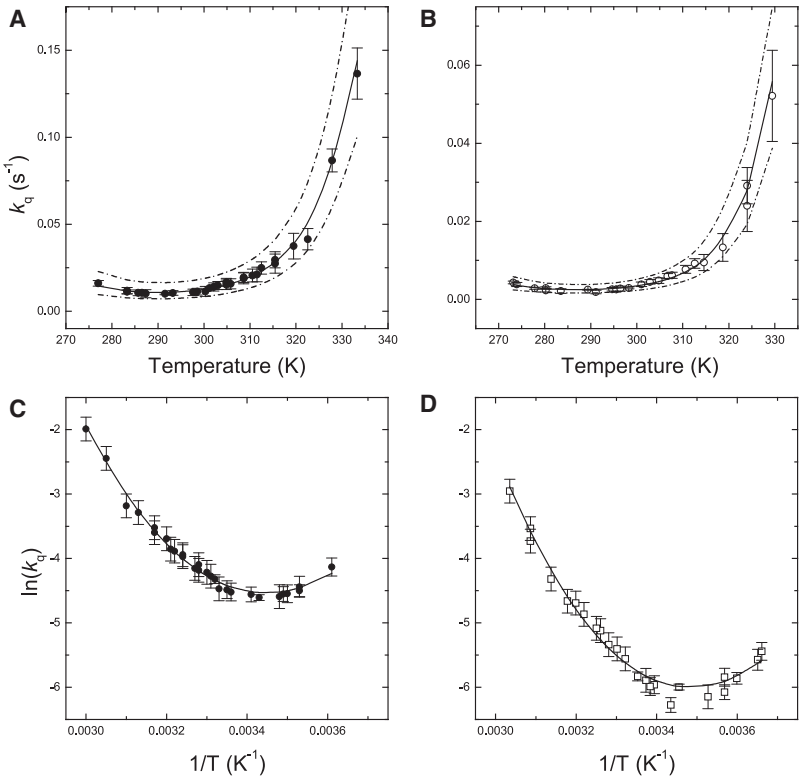


FIGURE 2 Temperature dependence of the rate of fluorescence quenching in LHCII monomers (*A*) and trimers (*B*). (*C* and *D*) Arrhenius plots of the experimental results shown on the panels *A* and *B*, respectively. (*Solid lines*) Best fits. (*Dashed lines*) Confidence interval ($2\sigma$). Errors bars as in the legend of Fig. 1.

the temperature dependence of the rate of fluorescence quenching in trimers and monomers of LHCII and their respective Arrhenius plots. The Arrhenius plots of the fluorescence quenching kinetics show an apparent discontinuity that occurs at higher temperature in LHCII trimers compared to monomers. The origin of this discontinuity is poorly understood (27,28). It was proposed to arise from a change in state of the complex, possibly connected to the conformational rearrangements occurring during the onset of singlet-excited state quenching. Discontinuous Arrhenius plots are not uncommon in studies concerning protein folding and unfolding (e.g., (29–34)). Formalism analogous to that commonly employed to describe large structural reorganization associated with protein folding can be extended to the predictably more restricted reconfiguration occurring during LHCII fluorescence quenching (Appendix S1 in the Supporting Material).

Inspecting the temperature dependence of the CD signal in LHCII monomers, it is possible to notice that the losses of intensity at 211 nm and 680 nm partially overlap on the temperature scale, so that the temperature-induced transitions to the quenched and unfolded states of the complex cannot be considered as independent. On the other hand, the overlap of the transitions is less pronounced in the case of LHCII trimers (Fig. 1). Hence, at least in LHCII trimers, the transitions to the quenched and the unfolded forms of the complex occur in a quasisequential manner. Using the assumption that the same reaction mechanism applies to monomers as well, we have investigated the experimental data by a linear three-stage kinetic scheme (Eq. 1) to which the data were fitted.

Remarkably, a good agreement (*solid lines* in Figs. 1 and 2) was found in the global analysis of the temperature dependencies monitoring either chromophore-chromophore interactions (680 nm) or protein secondary structure (211 nm) considering such a reaction scheme. In this scenario, the quenched state represents a folded intermediate between the (folded) unquenched and the unfolded states of LHCII. The temperature dependence of the quenching rate constant, as well as the discontinuous Arrhenius plots described by this relatively simple model, are also satisfactory. In this way, the thermodynamics of the transition to the quenched and the unfolded states are described by a few simple parameters: the quenching (melting) enthalpy differences $\Delta H_{q/m}$, the differences in heat capacity between the quenched and unquenched (unfolded and quenched) state $\Delta C_{p,q/m}$, and the characteristic quenching (melting) temperatures $T_{q/m}$, which are listed in Table 1. We notice that the values of $T_{q/m}$ are substantially model-independent, as they are virtually identical to those of previous reports (27,28) in which, however, $\Delta H^{\varnothing}$ and $\Delta C_p$ were not quantified. In Table 1, the values of $\Delta G_q^{\varnothing}$ (and $\Delta G_m^{\varnothing}$) are also shown for the room temperature. For both monomers and trimers of LHCII, the value of $\Delta G_q^{\varnothing}(RT)$ is within the 6.7–7 kJ $mol^{-1}$ interval, in a good agreement with the estimation obtained from the analysis of the quenching equilibrium in LHCII trimers as a function of the hydrostatic pressure, which yielded $\Delta G_q^{\varnothing}(RT) = 7.0 \pm 0.3$ kJ $mol^{-1}$ at the standard pressure (26). At room

**TABLE 1 Thermodynamic parameters of quenching and unfolding of LHCII**

| | Monomers | | Trimers | |
|---|---|---|---|---|
| Parameters | Quenching | Unfolding | Quenching | Unfolding |
| $\Delta H_i$ (kJ mol$^{-1}$) | 129 ± 5 | 152 ± 6 | 86.5 ± 2.9 | 404 ± 8 |
| $\Delta C_{p,i}$ (kJ mol$^{-1}$ K$^{-1}$) | 0.23 ± 0.11 | 4.9 ± 0.8 | 1.1 ± 0.2 | 7.8 ± 0.7 |
| $T_i$ (K) (°C) | 317.3 ± 0.5 (44) | 329 ± 1 (56) | 332 ± 0.7 (59) | 347 ± 1 (74) |
| $\Delta S_i$ (kJ mol$^{-1}$ K$^{-1}$) | 0.41 | 0.46 | 0.26 | 1.2 |
| $\Delta G(T_{RT})$ (kJ mol$^{-1}$) | 6.7 | 7.6 | 7.0 | 28.6 |
| $\Delta H^{\dagger}$ (kJ mol$^{-1}$) | −68.4 ± 2.1 | no data | 40.5 ± 1.5 | no data |
| $\Delta C_p{}^{\dagger}$ (kJ mol$^{-1}$ K$^{-1}$) | 2.7 ± 0.4 | no data | 1.8 ± 0.2 | no data |
| $\Delta S^{\dagger}$(kJ mol$^{-1}$ K$^{-1}$) | −0.48 ± 0.08 | no data | −0.14 ± 0.05 | no data |
| $K$ | 0.30 ± 0.05 | no data | 0.30 ± 0.06 | no data |
| $\Delta G^{\dagger}(T_q)$ (kJ mol$^{-1}$) | 83.8 | no data | 85.2 | no data |
| $\Delta G^{\dagger}(T_{RT})$ (kJ mol$^{-1}$) | 73.5 | no data | 77.4 | no data |

Thermodynamic parameters describing the steady-state levels and activation barriers of the quenching and the unfolding processes in monomers and trimers of LHCII. Also listed are the values of the free energy difference at room temperature $\Delta G(T_{RT})$.

temperature, the transition from the quenched to the unquenched form of the complex is only slightly endothermic (~2.5 the thermal energy). Thus, even though the two conformers are almost equally stable, it is the unquenched state that is favored. This finding provides further support for the choice of the linear model described by Eq. 1: it could be readily shown that an off-pathway reaction scheme can be translated into a linear scheme analogous to that described by Eq. 1, but in which the unquenched and quenched states interchange (Scheme S1A in the Supporting Material). Thus, it would be sufficient to redefine $\Delta G_m{}^{\varnothing}$ and $\Delta G_q{}^{\varnothing}$ (and the associated equilibrium constants) as the differences between the unfolded and unquenched states and the quenched and unquenched states, respectively. As $\Delta G_q{}^{\varnothing}(RT) > 0$, this would imply that the most thermodynamically favorable conformer (at room temperature) is the quenched state of LHCII. As it is well established that, at the room temperature, LHCII is mainly unquenched (e.g., (41–43)), the positive value of $\Delta G_q{}^{\varnothing}(RT) \approx 7$ kJ mol$^{-1}$, obtained by investigation of the effect of either pressure or temperature on the quenching equilibrium, is not consistent with the quenched form representing an off-pathway intermediate.

Finally, we would like to emphasize that, to describe the formation of the quenched state of LHCII, the differences in heat capacities between the relaxed and the quenched conformers ($\Delta C_{p,q}$) and the relaxed and the activated state conformers ($\Delta C^{\dagger}_{p,q}$) need to be distinct from zero. Although contribution of $\Delta C_p$ to $\Delta G^{\varnothing}(T)$ of protein folding is commonly reported (29–34), the observation of $\Delta C_p$ different from zero, for the most subtle conformational changes associated with the regulation of protein function has not been previously reported, at least to our knowledge. Nevertheless, this result is significant, as positive values of $\Delta C_p$ represent a characteristic marker of protein conformational rearrangements. It is noted that the magnitude of the $\Delta C_{p,q}$ term for trimers is almost fourfold larger than that of monomers. The value $\Delta C_{p,m}$ observed in LHCII trimers and monomers is within the range observed for the unfolding of soluble proteins of comparable molecular weight, whereas that of $\Delta C_{p,q}$ is on the lower end of the distribution of published values (31,33). The small value of $\Delta C_{p,q}$ reveals relatively contained rearrangements of the protein structure during the transition into the quenched state. Analogous conclusion was reached by the investigation of the pressure dependency of fluorescence quenching in LHCII trimers (26). The specific volume change upon the transition into the quenched form of LHCII (~0.006% of the trimer volume) was significantly smaller than the maximal pressure-induced volume compression (~3%).

## Thermal stability of the LHCII monomer and trimers and transition to the quenched and unfolded states of the complex

In the previous section, we have shown that a linear reaction scheme, in which the quenched conformer of LHCII represents a folded intermediate between the unquenched and the unfolded forms of the complex, is capable to describe the temperature dependences of the steady-state population levels of both the monomeric and the trimeric forms of LHCII. Nonetheless, the comparison of the thermodynamic parameters characterizing the transition to the quenched and the unfolded stets of LHCII demonstrate a remarkable effect of the oligomerization state of the complex. To visualize these differences we have plotted the molar fractions of unquenched ($\gamma_u$), quenched ($\gamma_q$), and unfolded ($\gamma_m$) states, extracted from the fitting of the experimental results, as a function of temperature in Fig. 3. The transitions to the quenched and to the unfolded states of the complex occur at lower temperatures in monomers ($T_q = 317$) with respect to the trimers ($T_q = 332$) (see also (27,28)). Fig. 3 also shows how the maximal molar fraction of quenched complexes ($\gamma_u$) reaches a higher steady-state level in LHCII trimers (~0.65) compared to monomers (~0.5). It should also be noticed that a significant fraction of LHCII monomers is already unfolded at the temperature at which quenching is not substantial in trimers.

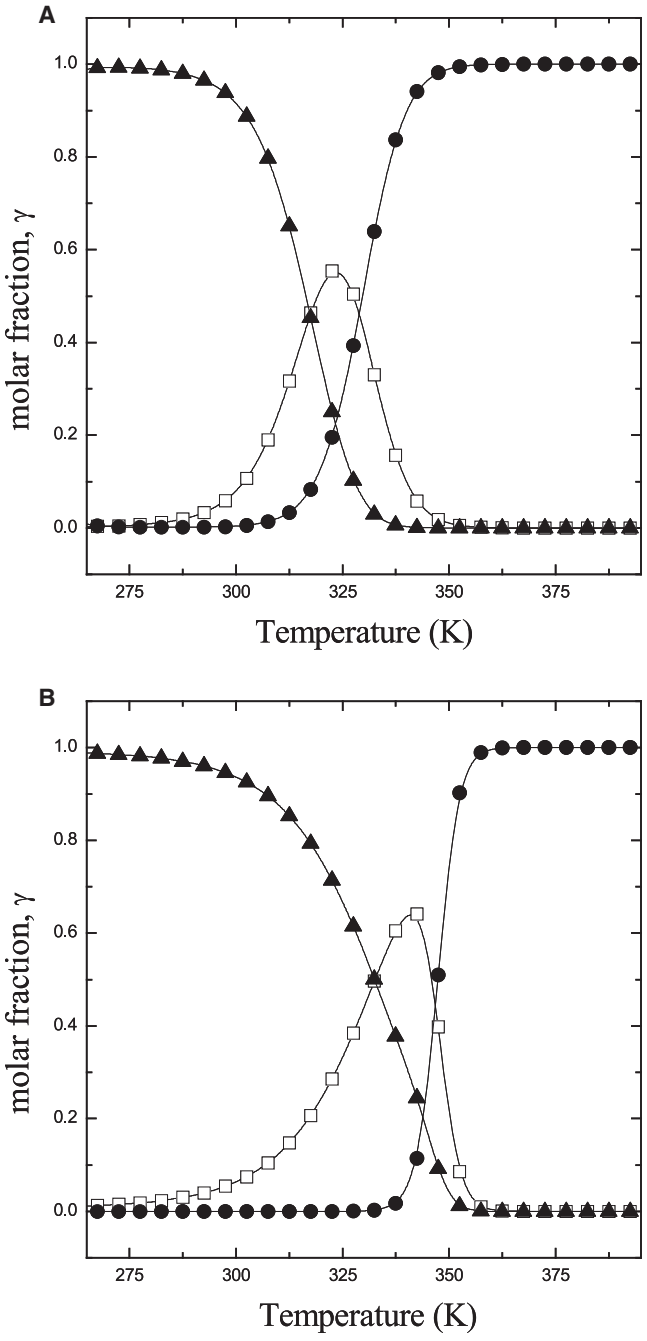


FIGURE 3 Temperature dependence of the molar fractions of unquenched (*solid triangles*), quenched (*open squares*), and unfolded (*solid circles*) LHCII complex computed from the fits to the experimental. (*A*) LHCII monomers; (*B*) LHCII trimers.

The unfolding transition displays a parallel increase in the characteristic melting temperature, $\Delta T_m^{Tr-Mn} = 22$ K, to that observed for the quenching transition, $\Delta T_q^{Tr-Mn} = 15$ K. This shows immediately that LHCII trimers are in a thermodynamically more stable configuration than monomers. The melting temperature of 329 ± 1 K (56°C) observed in monomers is not dissimilar from the average for many globular soluble proteins (33,44). On the other hand, the melting temperature of 347 ± 1 K (74°C) observed in trimers falls into the range of proteins isolated from a thermophilic organism (33,44).

## Cooperativity of the quenching and melting transitions

The plots of the molar fractions as a function of the incubation temperature (Fig. 3) show a more progressive and smooth transition of LHCII trimers into the quenched state in comparison to monomers (Fig. 3). This is a correlated to the value of $\Delta H_q^{\varnothing}$, which is an indicator of sharpness of the transition: $\Delta H_q^{\varnothing}$ is almost twofold larger in monomers (129.6 ± 5 kJ mol$^{-1}$) with respect to trimers (86.5 ± 3 kJ mol$^{-1}$).

The opposite behavior is observed during the transition into the unfolded state. In this case, a relatively cooperative transition is observed for LHCII monomers, for which $\Delta H_m^{\varnothing}$ equals 152 ± 6 kJ mol$^{-1}$. In contrast, a steep transition into the unfolded form in observed in LHCII trimers ($\Delta H_m^{\varnothing}$= 404 ± 8 kJ mol$^{-1}$). The enthalpy difference between the unfolded and folded conformers of monomeric LHCII is within the range of $\Delta H_m^{\varnothing}$ values reported for thermal denaturation of transmembrane proteins. In general, the values of $\Delta H_m^{\varnothing}$ reported for membrane protein unfolding compilation of values, see (31,33,44). On the other hand, for LHCII trimers $\Delta H_m^{\varnothing}$ equals 404 kJ mol$^{-1}$—a value that is rather large in absolute terms (31,33,44).

To a first approximation, $\Delta H^{\varnothing}$ scales linearly with the size of the domain(s) involved in a given conformational reconfiguration. The comparison of the $\Delta H_q^{\varnothing}$ and $\Delta H_m^{\varnothing}$ shows that in LHCII monomers the domains involved in the unquenched-to-quenched and the quenched-to-unfolded transitions have comparable dimensions. The protein domain(s) involved in unfolding undergoes a substantial increase in size upon trimerization based on the difference between $\Delta H_m^{\varnothing}$ (~400 kJ mol$^{-1}$) and $\Delta H_q^{\varnothing}$ (~86.5 kJ mol$^{-1}$). This is attributed to the stabilization of LHCII brought about by extensive, albeit weak, hydrophobic interaction at the monomer-monomer interfaces. This type of interactions in oligomeric structures is known to promote folding stabilization both in membrane (31) and in globular proteins (e.g., (45)).

## The thermodynamic stability of the unquenched and quenched forms of the LHCII trimer is due to compensation of entropic and enthalpic contribution to the Gibbs free energy difference

To get more insight into the thermodynamic parameters that determine the larger thermal stability of trimers with respect to monomers, the enthalpic ($\Delta H_q^{\varnothing}(T)$) and the entropic ($-T \times \Delta S_q^{\varnothing}(T)$) contributions to $\Delta G_q^{\varnothing}(T)$ were calculated and they are plotted in Fig. 4, where they are extrapolated to a temperature range larger than the experimental values to highlight the temperature dependencies. Fig. 4 shows that although the $\Delta G_q^{\varnothing}(T)$ profile is nearly constant and positive over a relatively large temperature range in

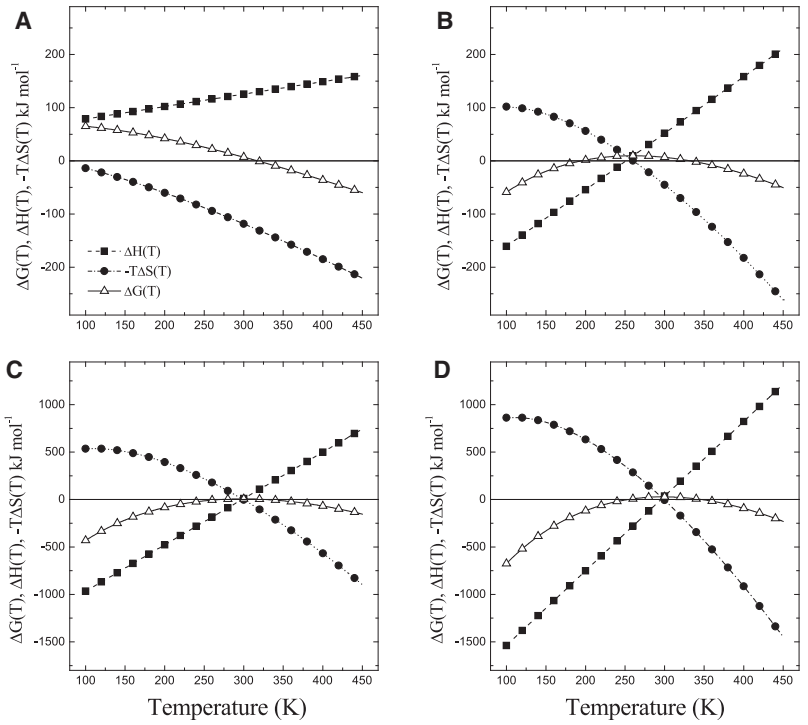


FIGURE 4 Temperature dependence of $\Delta G_q^{\varnothing}(T)$ (*open triangles*, *solid lines*), and its enthalpic, $\Delta H_q^{\varnothing}(T)$ (*solid squares*, *dashed lines*), and entropic, $-T\Delta S_q^{\varnothing}(T)$ (*solid circles*, *dotted lines*) terms for the conformational change associated with the quenching of LHCII monomers (*A*) and trimers (*B*). The temperature dependences of $\Delta G_m^{\varnothing}(T)$, $\Delta H_m^{\varnothing}(T)$, and $-T\Delta H_m^{\varnothing}(T)$ (unfolding process) of monomers (*C*) and trimers (*D*).

LHCII trimers, it is clearly temperature-dependent in monomers.

In the case of monomers, $\Delta H_q^{\varnothing}(T)$ is nearly temperature-independent due to the small value of $\Delta C_{p,q}$. As a result, the temperature dependence of $\Delta G_q^{\varnothing}(T)$ is almost entirely determined by the entropic term $T\Delta S_q^{\varnothing}(T)$. As the latter term increases almost linearly with temperature, it becomes dominant when $T >$ ~310 K (Fig. 4 *A*) so that the transition into the quenched form of the complex is entropy-driven.

In the case of trimers, $\Delta H_q^{\varnothing}(T)$ and $\Delta S_q^{\varnothing}(T)$ display a more pronounced temperature dependence (Fig. 4), stemming from the relatively larger value of $\Delta C_{p,q}$. Since $\Delta C_{p,q} > 0$, $\Delta H_q^{\varnothing}(T)$ increases linearly with temperature. On the other hand, $-T \times \Delta S_q^{\varnothing}(T)$ tends to decrease almost (asymptotically) linearly when $T \geq T_q$. Thus, the weak temperature dependency of $\Delta G_q^{\varnothing}(T)$ observed in LHCII trimers can be rationalized by the compensation of the entropic and enthalpic contributions to the free energy.

The values of $\Delta G_m^{\varnothing}(T)$, $\Delta H_m^{\varnothing}(T)$, and $T\Delta S_m^{\varnothing}(T)$ associated with the unfolding of LHCII are also reported in Fig. 4. The thermal stability of LHCII trimers could be explained by the same effect of compensation of entropy and enthalpy differences, due to the larger value of $\Delta C_{p,m}$ in trimers (~7.8 ± 0.7 kJ mol$^{-1}$ K$^{-1}$) compared to monomers (4.9 ± 0.8 kJ mol$^{-1}$ K$^{-1}$). Similar compensatory effects of entropic and enthalpic terms have been previously observed in folding studies of globular proteins where they were shown to correlate with protein thermal stability (46). Interestingly, here we show that similar thermodynamic features can be extended to a more subtle conformational rearrangement associated with functional states of proteins.

## Thermodynamic characterization of the transition state

The reinvestigation of the temperature dependence of the kinetics of LHCII fluorescence quenching (Fig. 2) demonstrated that, when the temperature dependence of $\Delta G_q^{\dagger}$ is taken into account, there is no need to adopt the ad hoc assumption of two processes occurring before and after a threshold temperature, as discussed previously (27,28). We show that all data can be explained by the unique properties of the conformational transition between the unquenched and the quenched state of LHCII complex. From this analysis (see also Table 1), it is possible to abstract the activation free energy of the exergonic (relaxation of the quenched state, $\Delta G_q^*(T)$), and that of the endergonic (formation of quenched state, $\Delta G_q^*(T)$) reactions, which are shown in Fig. 5 and compared with $\Delta G_q^*(T)$.

The total activation barrier for the unquenched-to-quenched transition is ~70–85 kJ mol$^{-1}$ either in monomers or trimers of LHCII (Fig. 5). The value of $\Delta G_q^*(T)$ is large compared to $\Delta G_q^{\varnothing}(T)$. The latter lays between −2 and 16 kJ mol$^{-1}$ for monomers and between 0.8 and 9 kJ mol$^{-1}$ for trimer of LHCII across the investigated temperatures. Thus, within physiologically relevant scenarios, the conformational switch between the unquenched and the quenched forms of the complex is controlled by the population of the transition state intermediate that is highly endergonic. Modulation of the energy barrier by allosteric effectors, such as ΔpH and binding of zeaxanthin (reviewed in (1–4,16)), can simply control the population of quenched LHCII complexes under conditions promoting NPQ in vivo.

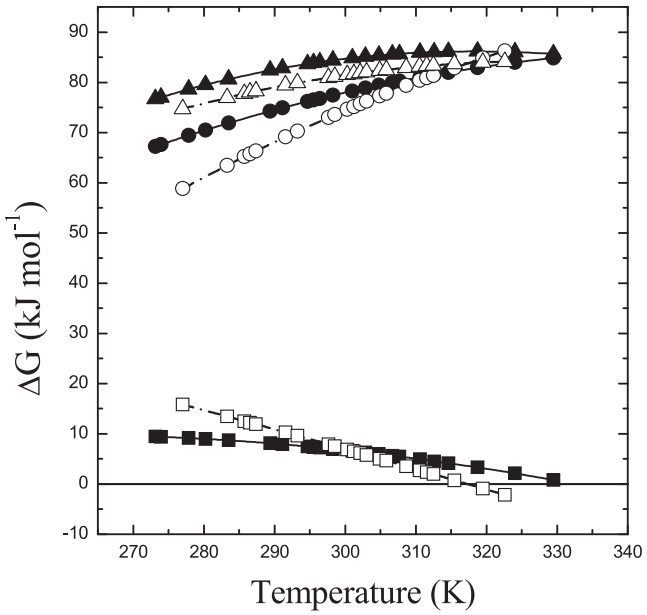


FIGURE 5 Temperature dependence of the free activation energy, $\Delta G_q^*$, for LHCII trimers (*solid triangles*) and monomers (*open triangles*). Also shown are the temperature dependences of $\Delta G_q^{\dagger}$ (*circles*) and that of $\Delta G_q^{\varnothing}(T)$ (*squares*). (*Solid symbols*) Trimers. (*Open symbols*) Monomers.

Yet, although the total activation barrier has similar magnitude in monomers and trimers of LHCII (Fig. 5), the relative contribution of the activation enthalpy, $\Delta H_q^{\dagger}$, and entropy, $\Delta S_q^{\dagger}$, differences from $\Delta G_q^{\dagger}$ are distinct in the two conformers. In LHCII monomers, $\Delta H_q^{\dagger}$ is negative and equals $-68.4 \pm 2.1$ kJ mol$^{-1}$. Negative values of activation enthalpy difference, for more extensive polypeptide reconfiguration associated with folding, were previously reported (47). Nonetheless, by virtue of a larger, positive value of $\Delta H_q^{\dagger}$ ($129 \pm 5$ kJ mol$^{-1}$), the endothermic transition has a positive activation enthalpy, $\Delta H_q^{\dagger} = \sim 60$ kJ mol$^{-1}$. Still, in LHCII monomers, a significant contribution to $\Delta G_q^{\dagger}(T)$ is provided by a relatively large, negative activation entropy difference, $\Delta S_q^{\dagger}$, of $-0.48 \pm 0.08$ kJ mol$^{-1}$ K$^{-1}$. In LHCII trimers, the enthalpy of activation is approximately double that of monomers, $\Delta H_q^{\dagger} = 120$ kJ mol$^{-1}$, partially because of the positive value of $\Delta H_q^{\dagger}$ (40 kJ mol$^{-1}$). On the other hand, $\Delta S_q^{\dagger}$ is approximately one-third that of monomers ($-0.13 \pm 0.05$ kJ mol$^{-1}$ K$^{-1}$).

Interestingly, both in LHCII monomers and trimers, the sign of $\Delta S_q^{\dagger}$ is negative. This can be taken as an indication that the transition state possesses a restricted degree of freedom compared to both the relaxed and the quenched LHCII conformers. A relatively wide landscape of possible transition state conformers is typically discussed for protein folding, and computational investigation have been performed for small globular polypeptides (e.g., (48–50)). The negative value of $\Delta S_q^{\dagger}$ points toward the existence of a defined intermediate in the transition between the unquenched and quenched form of the complex, rather than a pure transition state, which is unresolved due to temporal resolution of the measurement (see (32,38,50) for discussions relating to intermediate in protein folding).

## A model for conformational changes associated with the excited-state quenching in LHCII

The analysis of the unfolding and quenching transition of the LHCII complex shows a striking parallelism between the increase in the value of characteristic transition temperature, ($T_q$, $T_m$), and the differential heat capacities, ($\Delta C_{p,q}$, $\Delta C_{p,m}$), in trimers compared to monomers. This result is in accordance with a survey of soluble proteins from thermophilic and metaphilic organisms, which demonstrated an empirical correlation between the increase of $\Delta C_{p,q}$, $T_m$ and thermal stability (44). This observation tends to point toward the involvement of the same (or overlapping) domains of the protein in conformational reorganization, which promote quenching and unfolding of LHCII. Although the specific protein motifs involved in the process are not directly identified in this study, the modification of the environment of amino-acid residues taking part in the trimerization of LHCII appears to play a key role in both quenching and unfolding. Trimerization takes place mainly by hydrophobic interactions, involving a large number of residues of the large N-terminal domain, the stromal end of $\alpha$-helix *B*, and some residues of $\alpha$-helix *C*, as well as phospholipids and chlorophylls (Chl *a* 603, 613, 614, Chl *b* 601, 607, 609). Because of the rather hydrophobic character to the intermonomer interface, it can be hypothesized that the exposure of nonpolar side chains to the more polar bulk environment is involved in the conformational reorganization leading to singlet quenching in LHCII. This type of interaction is known to play a major role in the stabilization of globular proteins (e.g., (29–34)). Thus, for example, the induction of quenching by incubation of LHCII in the medium in which detergents are present at concentrations lower than critical micellar concentration can be explained in terms of the disappearance, or perturbation, of the relatively hydrophobic shield provided by the detergent micelles, so that the exposure to the solvent of nonpolar residues becomes less unfavorable. The increased hydrophobicity at the helix interfaces occurring as a result of trimerization will then explain the larger value of $\Delta C_{p,m}$ for this state of the complex compared to monomers, as more heat needs to be absorbed from the thermalized environment to promote the exposure of nonpolar side chains to the (polar) bulk solvent. It is also worth taking into account that LHCII monomers are produced by treatment of trimers with lipase (36). The influence of specifically bound and bulk membrane lipids can also be significant in the quenching and temperature stabilization processes.

## Comparison between the thermodynamic properties of LHCII in detergent micelles and in thylakoid membranes

Finally, we compare our results with studies of the temperature-induced reorganization of the thylakoid ultrastructure

and denaturation of LHCII embedded in native membranes (51). Investigation by means of differential scanning calorimetry (DSC) characterized several transitions occurring at 43–48°C, ~70°C, ~80°C, and ~90°C (52,53). All the processes occurring above 70°C were assigned to unfolding of photosynthetic Chl-binding complexes, including LHCII. In vitro we only resolved a single unfolding transition, which, in the case of trimers, is characterized by $T_m = 74$°C. It is possible that, due to the upper limit of the temperature range investigated in our study, the melting temperature determined in vitro represents an average between two unresolved transitions corresponding to the ~70°C and ~80°C peaks observed in thylakoids. However, even though LHCII is the most abundant polypeptide of the thylakoids, it is equally possible that processes other than LHCII unfolding alone contribute to the DSC thermograms. In view of such uncertainties, the results obtained in vivo and in vitro, agree relatively well for the case of LHCII trimers. Our analysis shows that unfolding of monomers in vitro exhibit $T_m = 56$°C (Table 1). In thylakoids, the DSC transitions occurring below 70°C were assigned to disassembling of the granal ultrastructure (43–48°C) and successive monomerization of LHCII trimers (60°C). The thermal unfolding of LHCII monomers would then be contributing to the DSC transitions occurring at temperatures above 70°C, which are, at least, ~20°C upshifted with respect to the results obtained in vitro. A similar shift in the characteristic melting temperature is observed upon reconstitution of bacterial reaction centers in artificial liposomes with respect to detergent micelles (52). Native membrane and artificial liposomes had similar effect on thermal stability of *R. sphaeroides* reaction center (F. Böhles and S. Santabarbara, unpublished). Thus, the difference in the melting temperature of LHCII monomers observed in $\beta$-maltoside micelles and in thylakoids membranes seems to indicate that the environment in which monomeric antenna complexes are studied, in vitro, is relatively artificial.

## CONCLUSIONS

The characterization of basic thermodynamic properties ($\Delta G^{\varnothing}(T)$, $\Delta H^{\varnothing}(T)$, $\Delta C_p$) of the quenching and unfolding transition of isolated LHCII highlights the physiological relevance of its trimeric structure. Firstly, trimerization stabilizes the unquenched form of the LHCII ensuring the optimization of light harvesting, as previously discussed by Wentworth et al. (27) and van Oort et al. (26). In addition, the trimeric structure stabilizes the quenched form of LHCII, with respect to the unfolded state as evinced from the larger, positive, value of $\Delta G_m^{\varnothing}(T)$. This is possibly important under physiological conditions since unfolded/misfolded states of antenna complexes are potentially harmful and have been shown to play an important role in photoinhibitory processes (53,54). Finally, trimerization seems to constrain the size of domain involved in the transition to the quenching state, as indicated by the low value of $\Delta H_q^{\varnothing}$. This results in a smoother transition between the unquenched and quenched conformers, which is likely to represent an important strategy to control and modulate the extent of singlet-excited quenching in PSII antenna, avoiding a rapid transition to the quenched, downregulated, and hence, less photochemically efficient state, of the PSII.

## SUPPORTING MATERIAL

Two appendices with equations, a scheme, and references are available at http://www.biophysj.org/biophysj/supplemental/S0006-3495(09)01060-1.

This work was supported by a Biotechnology and Biological Sciences Research Council grant No. BB/E009743/1 to A.V.R. S.S. was, in part, supported by a U.S. Department of Energy grant (No. DE-FG02-00ER15097).

## REFERENCES

1. Horton, P., A. V. Ruban, and R. G. Walters. 1996. Regulation of light harvesting in green plants. *Annu. Rev. Plant Mol. Biol.* 47:655–684.
2. Horton, P., and A. Ruban. 2005. Molecular design of the photosystem II light-harvesting antenna: photosynthesis and photoprotection. *J. Exp. Bot.* 56:365–373.
3. Niyogi, K. K. 1999. Photoprotection revisited. *Annu. Rev. Plant Physiol. Plant Mol. Biol.* 50:333–359.
4. Demmig-Adams, B. 1990. Carotenoids and photoprotection in plants: a role for the xanthophyll zeaxanthin. *Biochim. Biophys. Acta.* 1020:1–24.
5. Ruban, A. V., A. J. Young, and P. Horton. 1994. Modulation of chlorophyll fluorescence quenching in isolated light harvesting complex of photosystem II. *Biochim. Biophys. Acta.* 1186:123–127.
6. Ruban, A. V., and P. Horton. 1999. The xanthophyll cycle modulates the kinetics of nonphotochemical energy dissipation in isolated light-harvesting complexes, intact chloroplasts, and leaves of spinach. *Plant Physiol.* 119:531–542.
7. Jennings, R. C., G. Zucchelli, and R. Bassi. 1996. Antenna structure and energy transfer in higher plant photosystems. *In* Topics in Current Chemistry. J. Mattay, editor. Springer-Verlag, Berlin, Heidelberg.
8. Bassi, R., and S. Caffarri. 2000. LHC proteins and the regulation of photosynthetic light harvesting function by xanthophylls. *Photosynth. Res.* 64:243–256.
9. Jennings, R. C., F. M. Garlaschi, and G. Zucchelli. 1991. Light-induced fluorescence quenching in the light-harvesting chlorophyll a/b protein complex. *Photosynth. Res.* 27:57–64.
10. Barzda, V., R. C. Jennings, G. Zucchelli, and G. Garab. 1999. Kinetic analysis of the light-induced fluorescence quenching in light-harvesting chlorophyll *a/b* pigment–protein complex of Photosystem II. *Photochem. Photobiol.* 70:751–759.
11. Barzda, V., A. Istokovics, I. Simidjiev, and G. Garab. 1996. Structural flexibility of chiral macroaggregates of light-harvesting chlorophyll *a/b* pigment-protein complexes. Light-induced reversible structural changes associated with energy dissipation. *Biochemistry.* 35:8981–8985.
12. Liu, Z. F., H. C. Yan, K. B. Wang, T. Y. Kuang, J. P. Zhang, et al. 2004. Crystal structure of spinach major-light harvesting complex at 2.72Å resolution. *Nature.* 428:287–292.
13. Pascal, A. A., Z. Liu, K. Broess, B. van Oort, H. van Amerongen, et al. 2005. Molecular basis of photoprotection and control of photosynthetic light-harvesting. *Nature.* 436:134–137.
14. Ruban, A. V., A. A. Pascal, B. Robert, and P. Horton. 2001. Configuration and dynamics of xanthophylls in light-harvesting antennae of higher plants. Spectroscopic analysis of isolated light-harvesting complex of photosystem II and thylakoid membranes. *J. Biol. Chem.* 276:24862–24870.

15. Ruban, A. V., R. Berera, C. Illioaia, I. H. M. van Stokkum, T. M. Kennis, et al. 2007. A mechanism of photoprotective energy dissipation in higher plants. *Nature*. 450:575–578.

16. Robert, B., P. Horton, A. A. Pascal, and A. V. Ruban. 2004. Insights into the molecular dynamics of plant light-harvesting proteins *in vivo*. *Trends Plant Sci*. 9:385–390.

17. Holt, N. E., D. D. Zigmantas, L. Valkunas, X. P. Li, K. K. Niyogi, et al. 2005. Carotenoid cation formation and the regulation of photosynthetic light harvesting. *Science*. 307:433–436.

18. Avenson, T. J., T. K. Ahn, D. Zigmantas, K. K. Niyogi, Z. Li, et al. 2008. Zeaxanthin radical cation formation in minor light harvesting complexes of higher plant antenna. *J. Biol. Chem*. 283:3550–3558.

19. Ahn, T. K., T. Avenson, M. Ballottari, Y. C. Cheng, K. K. Niyogi, et al. 2008. Architecture of a charge-transfer state regulating light harvesting in a plant antenna protein. *Science*. 320:794–797.

20. Dexter, D. L. 1953. A theory of sensitized luminescence in solids. *J. Chem. Phys*. 21:836–850.

21. van Grondelle, R., J. P. Dekker, T. Gillbro, and V. Sundstrom. 1994. Energy trapping and transfer in photosynthesis. *Biochim. Biophys. Acta*. 1187:1–65.

22. Dreuw, A., and M. Wormit. 2008. Simple replacement of violaxanthin by zeaxanthin in LHCII does not cause chlorophyll fluorescence quenching. *J. Inorg. Biochem*. 102:458–465.

23. Garab, G., Z. Cseh, L. Kovács, S. Rajagopal, Z. Várkonyi, et al. 2002. Light-induced trimer to monomer transition in the main light-harvesting antenna complex of plants: thermo-optic mechanism. *Biochemistry*. 41:15121–15129.

24. Gulbinas, V., R. Karpicz, G. Garab, and L. L. Valkunas. 2006. Non-equilibrium heating in LHCII complexes monitored by ultrafast absorbance transients. *Biochemistry*. 45:9559–9565.

25. Ilioaia, C., M. P. Johnson, P. Horton, and A. V. Ruban. 2008. Induction of efficient energy dissipation in the isolated light-harvesting complex of Photosystem II in the absence of protein aggregation. *J. Biol. Chem*. 283:29505–29512.

26. van Oort, B., A. van Hoek, A. V. Ruban, and H. van Amerongen. 2007. Equilibrium between quenched and nonquenched conformations of the major plant light-harvesting complex studied with high-pressure time-resolved fluorescence. *J. Phys. Chem. B*. 111:7631–7637.

27. Wentworth, M., A. V. Ruban, and P. Horton. 2003. Thermodynamic investigation into the mechanism of the chlorophyll fluorescence quenching in isolated photosystem II light-harvesting complexes. *J. Biol. Chem*. 278:21845–21850.

28. Wentworth, M., A. V. Ruban, and P. Horton. 2004. The functional significance of the monomeric and trimeric states of the photosystem II light harvesting complexes. *Biochemistry*. 43:501–509.

29. Privalov, P. L. 1979. Stability of proteins. *Adv. Protein Chem*. 33:167–241.

30. Privalov, P. L., and S. J. Gill. 1988. Stability of protein structure and hydrophobic interaction. *Adv. Protein Chem*. 39:191–234.

31. Haltia, T., and E. Freire. 1995. Forces and factors that contribute to the structural stability of membrane proteins. *Biochim. Biophys. Acta*. 1241:295–322.

32. Dobson, C. M., and M. Karplus. 1999. The fundamental of protein folding: bringing together theory and experiment. *Curr. Opin. Struct. Biol*. 9:92–101.

33. Kumar, S., and R. Nussinov. 2001. How do thermophilic proteins deal with heath? *Cell. Mol. Life Sci*. 58:1216–1233.

34. Pace, C. N. 1990. Conformational stability of globular proteins. *Trends Biochem. Sci*. 15:14–17.

35. Ruban, A. V., A. J. Young, and P. Horton. 1996. Dynamic properties of the minor chlorophyll a/b binding proteins of photosystem II, an in vitro model for photoprotective energy dissipation in the photosynthetic membrane of green plants. *Biochemistry*. 35:674–678.

36. Nussberger, S., J. P. Dekker, W. Kühlbrandt, B. M. Bolhuis, R. van Grondelle, et al. 1994. Spectroscopic characterization of three different monomeric forms of the main chlorophyll a/*b* binding protein from chloroplast membranes. *Biochemistry*. 33:14775–14783.

37. Chen, B., W. A. Baase, and J. A. Schellman. 1989. Low-temperature unfolding of a mutant of phage T4 lysozyme. 2. Kinetic investigation. *Biochemistry*. 28:691–699.

38. Chan, H. S., and K. A. Dill. 1998. Protein folding in the landscape perspective: chevron plots and non-Arrhenius kinetics. *Proteins Struct. Funct. Genet*. 30:2–33.

39. Matagne, A., M. Jamin, W. Chung, C. V. Robinson, S. E. Radford, et al. 2000. Thermal unfolding of an intermediate is associated with non-Arrhenius kinetics of the folding of Hen Lysozyme. *J. Mol. Biol*. 297:193–201.

40. Beechem, J. M. 1992. Global analysis of biochemical and biophysical data. *Methods Enzymol*. 210:37–54.

41. Moya, I., M. Silvestri, O. Vallon, G. Cinque, and R. Bassi. 2001. Time-resolved fluorescence analysis of the photosystem II antenna proteins in detergent micelles and liposomes. *Biochemistry*. 40:12552–12561.

42. van Oort, B., A. van Hoek, A. V. Ruban, and H. van Amerongen. 2007. Aggregation of light-harvesting complex II leads to formation of efficient excitation energy traps in monomeric and trimeric complexes. *FEBS Lett*. 581:3528–3532.

43. Miloslavina, Y., A. Wehner, P. H. Lambrev, E. Wientjes, M. Reus, et al. 2008. Far-red fluorescence: a direct spectroscopic marker for LHCII oligomer formation in non-photochemical quenching. *FEBS Lett*. 582:3625–3631.

44. Kumar, S., C.-J. Tsai, and V. Nussinov. 2002. Maximal stabilities of two-state protein. *Biochemistry*. 41:5359–5374.

45. Luque, I., S. A. Leavitt, and E. Freire. 2002. The linkage between protein folding and functional co-operativity: two sides of the same coin? *Annu. Rev. Biophys. Biomol. Struct*. 31:235–256.

46. Shirtle, D., A. K. Meeker, and E. Freire. 1988. Stability mutants of staphylococcal nuclease: large compensating enthalpy-entropy changes for reversible denaturation reactions. *Biochemistry*. 27:4761–4768.

47. Oliveberg, M., Y. J. Tan, and A. R. Fersht. 1995. Negative activation enthalpies in the kinetics of protein folding. *Proc. Natl. Acad. Sci. USA*. 92:8626–8929.

48. Abkevich, V. I., A. M. Gutin, and E. I. Shakhovich. 1994. Free energy landscape for protein folding: intermediates, traps and multiple pathways in theory and lattice model simulations. *J. Phys. Chem*. 101:6052–6062.

49. Chapagain, P. P., J. L. Parra, B. S. Gerstman, and Y. Liu. 2007. Sampling the states for estimating the folding funnel entropy and energy landscape of a model $\alpha$-helical hairpin peptide. *J. Chem. Phys*. 127:075103–1/7.

50. Kim, P. S., and R. L. Baldwin. 1990. Intermediates in the folding reactions of small protein. *Annu. Rev. Biochem*. 59:631–660.

51. Dobrikova, A. G., Z. Várkonyi, S. Krumova, L. Kovács, G. K. Kostov, et al. 2003. Structural rearrangements in chloroplast thylakoid membranes revealed by differential scanning calorimetry and circular dichroism spectroscopy. Thermo-optic effect. *Biochemistry*. 42:11272–11280.

52. Böhles, F., M. Jones, and S. Santabarbara. 2007. Comparison of thermostability of reaction centers of R. *sphaeroides* in LDAO micelles and reconstituted into POCP liposomes. *In* Photosynthesis. Energy from Sun. J. F. Allen, E. Gant, J. H. Golbeck, and B. Osmond, editors. Springer, Dordrecht, The Netherlands.

53. Santabarbara, S., F. M. Garlaschi, G. Zucchelli, and R. C. Jennings. 1999. The effect of excited state population in photosystem II on the photoinhibition-induced changes in chlorophyll fluorescence parameters. *Biochim. Biophys. Acta*. 1409:165–170.

54. Santabarbara, S., K. V. Neverov, F. M. Garlaschi, G. Zucchelli, and R. C. Jennings. 2001. Involvement of uncoupled antenna chlorophylls in photoinhibition in thylakoids. *FEBS Lett*. 491:109–113.